NANO LETTERS

2002
Vol. 2, No. 2
97−100

Polyelectrolyte Hollow Sphere Lithographic Patterning of Surfaces: Construction of 2-Dimensional Well-Ordered Metal Arrays

Shubo Han, Xiangyang Shi, and Feimeng Zhou*

Department of Chemistry and Biochemistry, California State University, Los Angeles, Los Angeles, California 90032

Received September 24, 2001; Revised Manuscript Received November 17, 2001

ABSTRACT

Lithographic patterning of interconnected well-ordered metal arrays onto silicon wafers utilizing a 2-dimensional array of poly(diallyldimethylammonium chloride)/poly(sodium 4-styrenesulfonate) thin shells as the template is reported. The polyelectrolyte (PE) thin shells (hollow spheres) were produced by dissolving the polystyrene (PS) sphere cores. Structures of the arrays can be altered by varying the size of the PS spheres. The preparation of such arrays represents an inexpensive lithographic method for the fabrication of a variety of materials.

The fabrication of materials of micrometer- and submicrometer-sized patterns is of great scientific and technological importance in applications such as photonic materials,[1] microchip reactors,[2] miniaturized sensors,[3] and separation.[4] Colloidal crystals have been successfully used as templates for the creation of 3-dimensional (3D) macroporous materials.[1,4−8] Nanosphere lithography (NSL), on the other hand, has been demonstrated by Van Duyne and co-workers to be a highly versatile technique for producing well-ordered 2-D metallic nanoparticle arrays.[9] The two approaches bear a remarkable resemblance in that precursors or the final materials are filled in the interstitial space among the hexagonally close-packed nanospheres before the removal of the nanosphere mask. The major differences are that (1) the thickness of the filler material in NSL is much thinner (generally thinner than the diameter of the nanosphere) and (2) multilayers of nanospheres are more commonly used in the fabrication of macroporous materials.

Here we report a novel method for the construction of a 2-D well-ordered array of interconnected polyelectrolyte (PE) hollow spheres (shells) and a monolayer of conductive silver structure supported by the PE array. Our method differs from the aforementioned two approaches in that charged PE thin shells are used as the template. As a consequence, the precursor is not deposited in the hollow sphere interstices. Rather, they are infiltrated into the thin shells of the hollow spheres through the electrostatic attraction between the precursor and the outer PE surface. The production of interconnected features, instead of disconnected structures, was achieved because the PE shells remained in contact with one another upon the solvent extraction of the nanosphere cores. The preparation of such interconnected features thus affords new and alternative avenues for the lithographic patterning of surfaces with a wide range of charged inorganic and organic precursors.

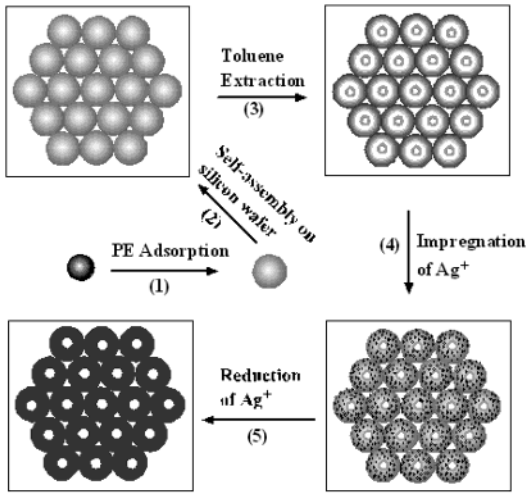

Figure 1. Schematic representation of the procedure for fabricating of PE thin shells and metal arrays.

Figure 1 depicts the procedure for the fabrication of the 2-D arrays of PE hollow spheres or shells, PE shells containing metal ions, and metallized PE shells. In step 1, the polystyrene nanospheres (PS, 640 or 1000 nm in

* Corresponding author. Phone: 323-343-2390; Fax: 323-343-6490; E-mail: fzhou@calstatela.edu.

10.1021/nl010071b CCC: $22.00
Published on Web 12/18/2001

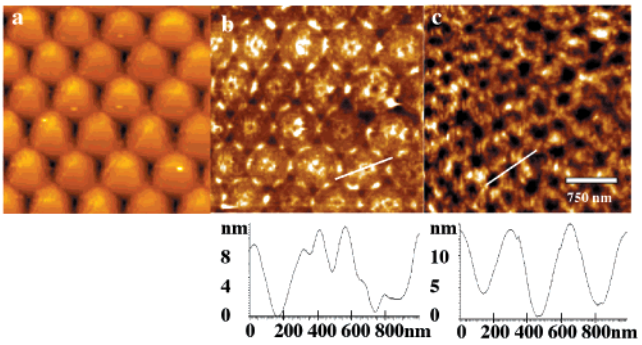

Figure 2. AFM images of silicon wafers covered with (a) a self-assembled monolayer of PE-coated PS nanospheres (core diameter = 640 nm); (b) an array of well-ordered thin PE (spheres) shells with their centers opened; and (c) a silver array produced from the electroless reduction of the impregnated Ag^+. The cross-sectional contours show the height variation of the thin PE shell array (image b) and that of the silver array (image c).

diameter, Interfacial Dynamics, Portland, OR) were coated with a poly(diallyldimethylammonium chloride)/poly(sodium 4-styrenesulfonate) (PDADMAC/PSS, Aldrich) bilayer through the layer-by-layer (LbL) technique. Specifically, this was accomplished by diluting 50 μL of the PS nanosphere solution to 1 mL with H_2O, followed by addition of 1 mL solution of PDADMAC (1 mg/mL in 0.5 M NaCl). After a 15-min adsorption, the excess PDADMAC was removed by three centrifuge (8500 rpm)/dispersion/washing cycles. A 1 mL portion of PSS solution (1 mg/mL in 0.5 M NaCl) was then added to the PDADMAC-modified PS sphere solution, followed by adsorption and removing steps similar as the PDADMAC deposition. In step 2, the PE-coated PS nanospheres were assembled onto a silicon wafer (Silicon Valley Microelectronics, Inc., San Jose, CA) by casting 25 μL of the nanoparticle solution onto the substrate and allowing the solvent to evaporate. The PS cores were then extracted from the surface by immersing the silicon wafer in toluene for 12 h (step 3). This step left well-ordered interconnected PDADMAC/PSS thin shells on the surface. Due to the negative charges on the outer PSS layer, metal ions such as Ag^+ can be infused into the thin shells upon exposure to a solution of the metal salt (step 4). To form the Ag array, the surface covered with the PDADMAC/PSS thin shells was exposed to a 0.6 M $AgNO_3$ solution overnight, followed by rinsing with water to remove unadsorbed Ag^+. Ag^+ penetrated into the PE shell was then converted to Ag through the use of the Tollen's reagent (step 5), in a manner similar to that reported by Xia et al.[10a]:

$$RCHO + 2Ag(NH)_3OH \rightarrow RCOO^- + 2Ag(s) + NH_4^+ + NH_3 + H_2O \quad (1)$$

Figure 2a displays a typical AFM (Molecular Imaging, Phoenix, AZ) image of the self-assembled PDADMAC/PSS-coated PS nanospheres (PS core diameter = 640 nm). These nanospheres formed a well-ordered close-packed monolayer after solvent evaporation. An average diameter of 688 ± 38 nm was deduced from the cross-sectional contour of the image. Since the thickness of PDADMAC/PSS films is ca. 4 nm,[11] the greater-than-expected difference between the diameters of PE-coated and uncoated spheres may originate from the imaging broadening effect due to the AFM tip interaction with the somewhat lossy PE layers.[12] Figure 2b shows the change occurred at a surface similar to that in Figure 2a after the dissolution of the PS cores. As can be seen, the PE thin shells remained on the substrate surface. As indicated by the cross-sectional contour of Figure 2b, the average thickness of the thin shell is about 12 nm. Thus, it is apparent that the compression of the top half crust of the PE sphere to the bottom half resulted from the extraction of the PS core (8 nm would be the expected thickness if the top half completely collapsed). As a consequence, the array of the PE thin shells resembles interconnected donut-shaped or circular features formed from the compression of the hollow spheres. Interestingly, this PE thin shell array does not appear to expand or contract along the surface, since the density of the thin PE shell array (2.50 circles/μm^2) is essentially the same as that in Figure 2a (2.44 PS nanospheres/μm^2). It is interesting to note that the inner diameters of these circular features are rather even. The ruptured central opening has an average diameter of 73 ± 11 nm. It is worth mentioning that the central opening is not produced by the interaction of the AFM tip with the PE shell, because both contact-mode and tapping-mode AFM showed essentially the same image. Moreover, it is unlikely that any possible damage caused by the AFM tip would not produce such a regular pattern on the array surface. Also of interest is that the shape of the interstitial region is of an equilateral triangle whose average length is 108 ± 12 nm. Apparently, all the shells are interconnected to form a regular array with few defects.

We should point out that the opal of close-packed nanosphere assembly is generally fabricated by dissolving or calcinating the nanoparticles embedded in matrices of substances such as metal salts,[5b−c,6a] metal particles,[1,5a,5c,13] polymeric materials,[5a,7b,13c] nematic liquid crystals,[8g] metal alkoxide precursors,[8a,14] and evaporated or electroplated metal films.[1b,9] To our knowledge, this is the first example of the construction of 2-D well-ordered PE thin shells through the utilization of the PE-coated nanosphere template.

To demonstrate the versatility associated with the above 2-D network of thin PE shells for surface modification, silver ions were implanted into the structure. The incorporation of the metal cations is accomplished via the electrostatic attraction of the metal ions by the negative charges on the outer PE layer (i.e., PSS). Upon electroless reduction of metal ions (eq 1), a metallic network can be produced. Figure 2c displays a typical Ag-containing PDADMAC/PSS array. While the framework in Figure 2c resembles that in Figure 2b, the cavities of the central opening of and the interstices between the circles in Figure 2b have become indistinguishable. The average diameter of these holes is 101 ± 10 nm. The thickness of the silver network (14 ± 8 nm) is highly comparable to that of the compressed PE thin shell (12 nm). The effective size of the defect-free 2-D silver array was found to be greater than 70 μm^2. Such an area is comparable

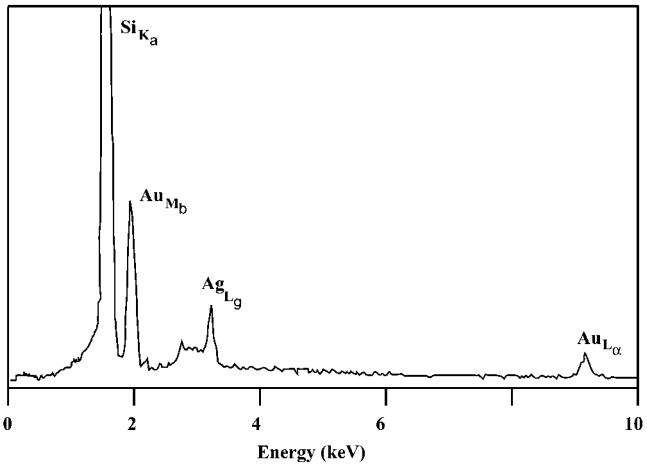

Figure 3. Typical energy dispersion X-ray spectrum collected from a surface similar to that shown in Figure 2c.

to that produced by typical NSL of discrete silver nanoparticle arrays (10−100 μm^2).[9a] The presence of silver in the PE scaffold was verified by the energy dispersion X-ray spectrometry (Figure 3). Note that the Au signals arose from the 2-nm Au coating sputtered onto the structure for the acquisition of a scanning electron micrograph (SEM) across a large area. It turned out that most of surface structures (e.g., features in Figures 2b and 2c) could not be well resolved by SEM (data not shown), owing to the very thin framework present at the silicon substrate. Coating a thin metal layer onto such a thin surface structure uniformly (a requirement for high-resolution SEM imaging) was challenging, since a delicate balance must be struck between the thinnest uniform coating achievable and an excessively thick coating that obscures surface details.[15] The unsatisfactory resolution of SEM for imaging of small quantities of thin films suggests that AFM is a more suitable technique for this application. Such a point has been made by Van Duyne and co-workers in their AFM characterization of fine NSL patterns.[9]

We also attempted to fabricate a silver array by extracting the PS cores after the electroless reduction of the infiltrated Ag ions (i.e., performing step 3 in Figure 1 as the final step). The resultant surface was found to contain many defects and to be poorly ordered (data not shown), due to the ineffective dissolution of the PS core through the PE-supported Ag structure.

Since PS nanoparticles with various sizes (0.02−10 μm)[10b] are commercially available, precisely tailoring the size of the 2-D array should be possible by coating PE shells onto different-sized nanospheres. Figure 4 depicts typical AFM images of the self-assembled PDADMAC/PSS-coated PS nanospheres (PS particle diameter = 1000 nm, panel a), the PDADMAC/PSS shell array (panel b), and the Ag-containing PDADMAC/PSS network (panel c). Evidently, the diameter of the PE-coated nanospheres (1060 ± 95 nm), the diameter of the central opening in the PE shell array (359 ± 30 nm), and the diameter of the holes in the Ag-containing PE shell (255 ± 20 nm) are all larger than the counterparts in Figure 2a−c arising from the PE-coated 640 nm-diameter PS

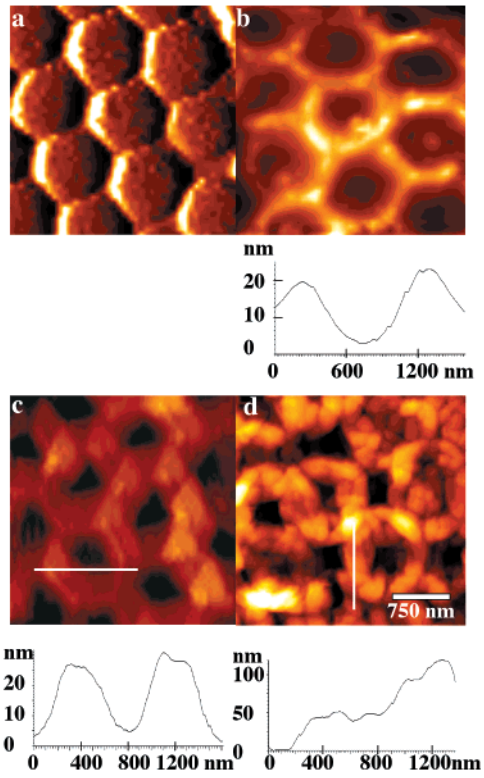

Figure 4. AFM images of silicon wafers covered with (a) a 2-D array of PS nanospheres (core diameter = 1000 nm), (b) well-ordered hollow PE spheres (shells), (c) a 2-D silver array, and (d) a multilayer of Ag rings, fabricated through the use of multilayered-shell-array template. The cross-sectional contours show the height variations of the PE shell array (image b), the monolayered silver array (image c), and the multilayered silver array (image d).

nanospheres. Likewise, both heights of the PE shells (20 ± 8 nm) and the silver array (25 ± 9 nm), shown by the cross-sectional contours, are also greater. Because the surface-to-volume is less for the larger PS spheres, the PE shells might be less mechanically stable toward the core dissolution. Consequently, the area of central opening in the PE shells becomes greater. This may explain why the circular opening in Figure 4b is greater than that in Figure 2b. Also worth noting is that the interstitial voids in Figures 4b and 4c, unlike their counterparts in Figures 2b and 2c, had been filled with PE. Thus, it seems that, when PS cores of larger diameters are used, the interstitial regions among the interconnected PE-coated PS spheres can be more easily filled.

Certain physical properties of the Ag-containing PE array were investigated. First, the mechanical stability of the array was found to be quite good, as subjecting the array to sonication for 10 min did not cause any peeling of the structure off the substrate. Second, the Ag imbedded in the PE backbone exhibited a relatively good chemical stability. Heating the array in a conventional oven at 60 °C for 2 h did not result in any noticeable color change. Only after a 4-h heating, was a slightly darker film (Ag_2O formation) observed. Finally, the Ag-containing PE array was found to be conductive. To measure the conductivity, we sputtered two gold bands onto a quartz substrate with a separation of 1.5 mm and made a pattern similar to that in Figure 4c to

bridge the gap between the two bands. A conductivity of 6.25−200 s/cm was determined. The conductivity is less than that of silver metal (6.45×10^5 s/cm)[16] but appears to be greater than the typical ion-doped macroporous conducting polypyrrole or polyaniline film.[17]

Finally, we demonstrate that multilayered Ag-impregnated PE networks can be fabricated by simply casting a more concentrated PE-coated PS nanosphere solution onto the silicon substrate. A representative AFM image of the PE-shell-supported silver array constructed in this fashion is shown in Figure 4d. Clearly the surface motif is analogous to that in typical macroporous materials synthesized by the nanosphere-template-directed method. In Figure 4d, while the inner diameter (ca. 267 ± 34 nm) is comparable to that in Figure 4c, the height variation (120 ± 45 nm) is significantly greater than that in Figure 4c (25 ± 9 nm). The image shows that some of the interconnected Ag/PE rings are stacked together. Some irregular pores between the stacked rings are also discernible in Figure 4d.

In summary, the combination of colloidal templating, LbL deposition of PE, and the assembly of the PE-coated colloidal particles onto a surface resulted in the formation of a monolayer or multilayers of interconnected PE thin shells or rings. These 2-D arrays or 3-D macroporous structures can further serve as new templates for the fabrication of other array surfaces composed of different materials. Coupled with the controllability inherent in the LbL method, tailoring the thickness (by altering the number of PE adsorption cycles) and the property of the shells (by changing the type of charged species) can be achieved straightforwardly. As a result, array surfaces of new types of materials should be derivable through a systematic and judicious variation of the compositions and sizes of the cores and the PE shells, the quantities of the resultant PE-coated nanospheres, and the species infusible into the PE shells or spheres. Experiments for examining various preparative parameters and for incorporating other charged species into the PE arrays are currently in progress.

Acknowledgment. Support from a NIH-SCORE grant (GM 08101) and an AREA grant (GM R15 63530-01) and the NSF-RUI (DBI-9978806) program is gratefully acknowledged.

References

(1) Jiang, P.; Cizeron, J.; Bertone, J. F.; Colvin, V. L. *J. Am. Chem. Soc.* **1999**, *121*, 7957−7958.
(2) Gau, H.; Herminghaus, S.; Lenz, P.; Lipowsky, R. *Science* **1999**, *283*, 46−49.
(3) (a) Taton, T. A.; Lu, G. L.; Mirkin, C. A. *J. Am. Chem. Soc.* **2001**, *123*, 5164−5165. (b) Fendler, J. H. *Chem. Mater.* **2001**, *13*, 3196−3210.
(4) Stein, A. *Microporous Mesoporous Mater.* **2001**, *44*−*45*, 227−239.
(5) (a) Jiang, P.; Bertone, J. F.; Colvin, V. L. *Science* **2001**, *291*, 453−457. (b) Turner, M. E.; Trentler, T. J.; Colvin, V. L. *Adv. Mater.* **2001**, *13*, 180−183. (c) Kulinowski, K. M.; Jiang, P.; Vaswani, H.; Colvin, V. L. *Adv. Mater.* **2000**, *12*, 833−838.
(6) (a) Holland, B. T.; Blanford, C. F.; Stein, A. *Science* **1998**, *281*, 538−540. (b) Blanford, C. F.; Schroden, R. C.; Al-Daous, M.; Stein, A. *Adv. Mater.* **2001**, *13*, 26−29. (c) Blanford, C. F.; Yan, H.; Schroden, R. C.; Al-Daous, M.; Stein, A. *Adv. Mater.* **2001**, *13*, 401−407.
(7) (a) Johnson, S. A.; Brigham, E. S.; Ollivier, P. J.; Mallouk, T. E. *Chem. Mater.* **1997**, *9*, 2448−2458. (b) Johnson, S. A.; Ollivier, P. J.; Mallouk, T. E. *Science* **1999**, *283*, 963−965. (c) Egan, G. L.; Yu, J. S.; Kim, C. H.; Lee, S. J.; Schaak, R. E.; Mallouk, T. E. *Adv. Mater.* **2000**, *12*, 1040−2.
(8) (a) Imhof, A.; Pine, D. J. *Nature* **1997**, *389*, 948−951. (b) Xia, Y.; Whitesides, G. M. *Annu. Rev. Mater. Sci.* **1998**, *28*, 153−184. (c) Wang, D.; Caruso, F. *Adv. Mater.* **2001**, *13*, 350−354. (d) Fleming, M. S.; Mandal, T. K.; Walt, D. R. *Chem. Mater.* **2001**, *13*, 2210−2216. (e) Srinivasarao, M.; Collings, D.; Phillips, A.; Patel, S. *Science* **2001**, *292*, 79−83. (f) Wijnhoven, J. E. G. J.; Vos, W. L. *Science* **1998**, *281*, 802−804. (g) Luther, B. J.; Springer, G. H.; Higgins, D. A. *Chem. Mater.* **2001**, *13*, 2281−2287. (h) Deutsch, M.; Vlasov, Y. A.; Norris, D. J. *Adv. Mater.* **2000**, *12*, 1176−1180. (i) Shiflett, M. B.; Foley, H. C. *Science* **1999**, *285*, 1902−1905. (j) Schuurmans, F. J. P.; Vanmaekelbergh, D.; van de Lagemaat, J.; Lagendijk, A. *Science* **1999**, *284*, 141−143.
(9) (a) Hulteen, J. C.; Van Duyne, R. P. *J. Vac. Sci. Techonol. A* **1995**, *13*, 1553−1558. (b) Haynes, C. L.; Van Duyne, R. P. *J. Phys. Chem.* **2001**, *105*, 5599−5611. (c) Jensen, T. R.; Malinsky, M. D.; Haynes, C. L.; Van Duyne, R. P. *J. Phys. Chem.* **2000**, *104*, 10549−10556. (d) Malinsky, M. D.; Kelly, K. L.; Schatz, G. C.; Van Duyne, R. P. *J. Am. Chem. Soc.* **2001**, *123*, 1471−1482.
(10) (a) Xia, Y.; Venkateswaran, N.; Qin, D.; Tien, J.; Whitesides, G. M. *Langmuir* **1998**, *14*, 363−371. (b) Xia, Y.; Gates, B.; Yin, Y.; Lu, Y. *Adv. Mater.* **2000**, *12*, 693−713.
(11) Caruso, F.; Lichtenfeld, H.; Donath, E.; Mohwald, H. *Macromolecules* **1999**, *32*, 2317−2328.
(12) Noy, A.; Vezenov, D. V.; Lieber, C. M. *Annu. Rev. Mater. Sci.* **1997**, *27*, 381−421.
(13) (a) Velev, O. D.; Tessierr, P. M.; Lenhoff, A. M.; Kaler, E. W. *Nature* **1999**, *401*, 548. (b) Tessier, P. M.; Velev, O. D.; Kalambur, A. T.; Rabolt, J. F.; Lenhoff, A. M.; Kaler, E. W. *J. Am. Chem. Soc.* **2000**, *122*, 9554−9555. (c) Velev, O. D.; Lenhoff, A. M.; Kaler, E. W. *Science* **2000**, *287*, 2240−2243.
(14) Manoharan, V. N.; Imhof, A.; Thorne, J. D.; Pine, D. J. *Adv. Mater.* **2001**, *13*, 447−450.
(15) Skoog, D. A.; Holler, F. J.; Nieman, T. A. *Principles of Instrumental Analysis*; Saunders College Publishing: Philadelphia, PA, 1998.
(16) Kittel, C. *Introduction to Solid State Physics*, 6th ed; John Wiley & Sons: New York, 1986.
(17) Bartlett, P. N.; Birkin, P. R.; Ghanem, M. A.; Toh, C. S. *J. Mater. Chem.* **2001**, *11*, 849−853.

NL010071B